Soil & Tillage Research 260 (2026) 107103

Contents lists available at ScienceDirect

Soil & Tillage Research

journal homepage: www.elsevier.com/locate/still

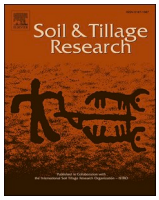

Within-field variation in root-to-shoot ratios and root traits in spring barley: Implications for estimating carbon inputs

Miyanda Chilipamushi [a,*], Claudia von Brömssen [b], Tino Colombi [a,c], Thomas Kätterer [d], Mats Larsbo [a]

[a] Department of Soil and Environment, Swedish University of Agricultural Sciences, Box 7014, Uppsala 750 07, Sweden
[b] Department of Energy and Technology, Swedish University of Agricultural Sciences, Box 7013, Uppsala 750 07, Sweden
[c] School of Biosciences, University of Nottingham, Sutton Bonington LE12 5RD, UK
[d] Department of Ecology, Swedish University of Agricultural Sciences, Box 7044, 750 07 Uppsala, Sweden

ARTICLE INFO

Keywords:
Allometric functions
Root-to-shoot ratio
Soil carbon inputs
Soil carbon modelling
Soil organic carbon monitoring
Temporal variability
Within-field variability

ABSTRACT

Roots are a major pathway for carbon (C) input into agricultural soils, yet field-scale measurements of below-ground C inputs and associated root traits remain limited. Consequently, many soil carbon models rely on fixed root-to-shoot ratios, and root trait variability is rarely considered. In this study, we quantified within-field variation in root-to-shoot ratios and root traits (root diameter, root length density and root tissue density) in spring barley (*Hordeum vulgare* L.) grown in southwestern Sweden in soil classified as Stagnic Eutric Cambisol, Eutric Stagnosol or Haplic Phaeozem according to the World Reference Base system. Roots (0–40 cm) and shoots were sampled during early to mid-reproductive stage, i.e. milking/early dough development stage, in a 50 × 50 cm grid at 11 sampling locations in the same field in two consecutive years. Shoot and root biomass were not correlated, resulting in variable root-to-shoot ratios (quartile coefficients of variation 7–18 %) and no consistent spatial pattern between years. Root traits displayed clear between year and depth variation, with coarser roots in the topsoil and root tissue densities and root length densities shifting across the profile, reflecting the highly plastic nature of root systems. The spatial variation in root properties in the field could not be explained by basic soil properties. Our findings call for a more mechanistic understanding of the drivers for root-to-shoot ratios and the plastic response of root traits to improve field-scale estimates of root-derived C inputs and SOC modelling accuracy.

1. Introduction

Changes in soil organic carbon (SOC) stocks in agricultural soils are monitored using repeated soil inventories or estimated with dynamic soil carbon models such as RothC (Coleman and Jenkinson, 2014), C-TOOL (Taghizadeh-Toosi et al., 2014), ICBM (Bolinder et al., 2019) and Yasso07 (Liski et al., 2005). In arable crops, about 25 % of the carbon fixed through photosynthesis is allocated to roots and rhizodeposition (Jacobs et al., 2020). Root-derived carbon inputs are particularly important for carbon balances, as they tend to form more stable SOC pools compared to input from above-ground plant residues (Rasse et al., 2005, Kätterer et al., 2011, Gasser et al., 2022). Hence, SOC input through roots needs to be properly accounted for in monitoring programs and modelling efforts. However, root sampling and analysis are labor-intensive, and root data are, therefore, often limited (Böhm, 1979, Cabal et al., 2021, Lux and Rost, 2012). Although above- and especially below-ground plant traits play a key role in determining SOC inputs, their influence on overall SOC balances remains insufficiently explored. Consequently, soil carbon models rely on simplifications such as fixed root-to-shoot ratios to estimate root-derived carbon inputs. This introduces uncertainty in modelled soil carbon inputs because, in reality, root-to-shoot ratios vary with soil properties, soil and crop management, soil nutrient status, soil moisture and climate (Bolinder et al., 2007, Taghizadeh-Toosi et al., 2020).

Previous studies have primarily focused on soil and crop management effects on root-shoot ratios using long-term plot-scale field experiments (Xu and Juma, 1992) and on inter-field and regional variability in root-to-shoot ratios (Bolinder et al., 2007, Mattila and Häkkinen, 2025, Hirte et al., 2018, Plaza-Bonilla et al., 2013, Heinemann et al., 2025) with little consideration of field scale heterogeneity.

* Corresponding author.
E-mail address: miyanda.chilipamushi@slu.se (M. Chilipamushi).

https://doi.org/10.1016/j.still.2026.107103
Received 17 September 2025; Received in revised form 1 February 2026; Accepted 3 February 2026
Available online 7 February 2026

Furthermore, it remains difficult to separate the effects of soil properties from the effects of management and climate in regional studies since this would require large amounts of data. For example, regional studies of annual crops have shown that root-to-shoot ratios may vary with soil texture (Poeplau and Kätterer, 2017; Mattila and Häkkinen, 2025) and weather conditions (Hirte et al., 2021).

Soil carbon sequestration is not determined by the quantity of root input only. The root system architecture (i.e., the spatial configuration of the root system), which encompasses features such as root length, spread, and diameter (Khan et al., 2016), influences microbial accessibility and, hence, root turnover. Despite the impact of above- and particularly below-ground plant traits for estimating SOC inputs, their impacts on SOC balances are understudied (Raza et al., 2025). Similar to root-to-shoot ratios, root architecture exhibits substantial variation in response to soil and crop management, soil properties and climate (Bao et al., 2014, Weemstra et al., 2022, Weemstra et al., 2021, Asefa et al., 2022, Durand-Maniclas et al., 2025). Soil-crop simulation models (e.g. USSF (Jarvis et al., 2024); DAISY (Hansen et al., 2012); APSIM (O'Leary et al., 2015)) are increasingly used to simulate SOC dynamics and other ecosystem processes under varying environmental and management conditions. These models integrate key biophysical processes such as crop growth, water and nutrient uptake, and carbon allocation, and often also consider, at least some aspects of root system architecture, such as root length density and diameter (Seidel et al., 2024, Dupuy et al., 2010). A deeper understanding of within-field variation in root architecture and its interaction with soil properties, as well as examining both between- and within-field variability in the root-to-shoot ratio and its underlying drivers, could enable improved process descriptions and parameterization of belowground components in soil and crop, and SOC models (Dupuy et al., 2010, Raza et al., 2025).

The objectives of this study were to i) quantify the within-field spatial and between year variation in shoot and root properties and corresponding root-to-shoot ratios, ii) quantify the within-field variation in root traits such as the root diameter, root length density and root tissue density, iii) test if soil properties could explain the variation in shoot and root properties, and iv) test if root biomass could explain the within-field variation in SOC in the topsoil. This was achieved by collecting shoot and root samples of spring barley during early to mid-reproductive stage, i.e. milking/early dough development stage from 11 sampling points during two consecutive years in a commercially managed field with large variation in soil texture and SOC content. This study moves beyond "average" rooting and biomass allocation by quantifying spatial heterogeneity within a single field and by linking root-to-shoot ratios and root traits to within-field variation in soil properties that are generally not considered in regional studies or in long-term plot-scale field experiments.

2. Methods and materials

2.1. Site description

The study area was a 46.9 ha conventionally-managed field in Bjertorp, Västergötland, in southwestern Sweden (58°14'00"N 13°08'00" E) with large spatial variations in soil texture and SOC content (clay content 9–45 % and SOC content 0.6–2.7 g kg^{-1} in the topsoil (0–20 cm) (Lindahl et al., 2008). Mean annual precipitation and temperature between 1961 and 2024 were 706 mm and 6.8°C, respectively. Depending on location, the soil in the field was classified either as Stagnic Eutric Cambisol, Eutric Stagnosol or Haplic Phaeozem according to the World Reference Base system (IUSS Working Group, 2015, Fukumasu et al., 2021). The field has been under continuous arable cultivation for more than 60 years (Lindahl et al., 2008, Fukumasu et al., 2021). The crop rotation has primarily consisted of winter wheat (*Triticum aestivum)*, barley (*Hordeum vulgare* L), oats (*Avena sativa*) and oilseed rape (*Brassica napus* L) as the main crops. The uppermost 20–25 cm has been mouldboard ploughed in the autumn, with a shallower plough depth in years when winter rapeseed was sown (Fukumasu et al., 2021). Fertilization has been applied with nitrogen, phosphorus, and potassium, with no addition of farmyard manure (Fukumasu et al., 2021). Fertilizers were applied at sowing between seeding rows at rates of 70, 26 and 44 kg ha^{-1} of nitrogen, phosphorus and potassium in 2023, and 70, 32 and 52 kg ha^{-1} of nitrogen, phosphorus and potassium in 2024. Additional nitrogen fertilizer was applied uniformly to the soil surface at 24 kg ha^{-1} in 2023 and 43 kg ha^{-1} in 2024.

2.2. Sampling design and analyzed variables

The sampling locations were selected to cover the variation in SOC content and soil texture (Fig. 1A, B). This selection was based on data from Fukumasu et al. (2021), who investigated the relationships between soil physicochemical properties, the reactive mineral phase, mean relative grain yield (as a proxy for carbon input) and SOC content in different soil fractions. From the initial 35 sampling points selected by Fukumasu et al. (2021), we applied systematic sampling at a fixed interval based on the SOC content analyzed by Fukumasu et al. (2021) to obtain the 11 representative sampling points shown in Fig. 1A, from which we collected samples for the analysis here. We sorted the SOC content measurements for the 35 points in ascending order and selected every third point.

Soil samples at the same sampling points were previously collected and analyzed by Fukumasu et al. (2021) for the variables listed in Table S1 at a depth of 3 – 13 cm. From the published dataset, we used SOC content, clay content, and elevation (Table 1). The elevation was between 88 and 94 m above sea level with a median slope of 0.3°. Loose soil was sampled at about 3 – 13 cm, dried at 38℃, crushed and sieved to < 2 mm, and SOC content was subsequently determined using a LECO Trumac CN analyzer according to SS-ISO 10694 (Fukumasu et al., 2021). Soil texture was also analyzed using the pipette method after organic matter oxidation according to Messing et al., 2024 in the data published in Fukumasu et al., 2021. A full description of the methods can be found in Fukumasu et al. (2021). Precipitation and temperature data at a daily resolution were obtained from a gridded map produced by the Swedish Meteorological and Hydrological Institute (SMHI) for the two years of our study (2023 and 2024).

2.3. Crops and growth conditions

Two-rowed spring barley (*Hordeum vulgare* L.) was grown in both 2023 and 2024 using different cultivars in the two years (Laureate in 2023 and Lexy in 2024). Plants were sampled during early to mid-reproductive stage, i.e. milking/early dough development stage (BBCH 71–83) in both years to capture root biomass after flowering, even though maximum biomass is often reported to occur at flowering (Gregory et al., 1996; Hoad et al., 2001) and to avoid the presence of extraneous organic matter (Hirte et al., 2017; Watt et al., 2008). Lexy and Laureate are similar malting barley cultivars; Lexy is distinguished by fine straw, while Laureate has a slightly shorter stalk (Lantmännen, 2025). In 2023, the plants were sown on 21st April. Root and shoot samples were collected on 25th and 26th July 2023. The mean temperature between sowing and sampling was 12.7 °C, and average daily precipitation during the same time was 2.6 mm, with a maximum daily precipitation of 37.3 mm. Cumulative precipitation in the preceding months was also relatively low compared to the peak in August (192.3 mm; Fig. 1D). Throughout the growing period, average monthly temperatures remained below 20 °C (Fig. 1C).

In 2024, plants were sown on 13th May. Root and shoot sampling were carried out on 29th and 30th July 2024 with a mean temperature of 12.7 °C and an average daily precipitation of 2.4 mm between sowing and sampling. Cumulative precipitation in April 2024 was approximately six times higher than in April 2023, and precipitation in the following two months was also larger in 2024 (Fig. 1D). Average monthly temperatures did not exceed 20 °C (Fig. 1C).

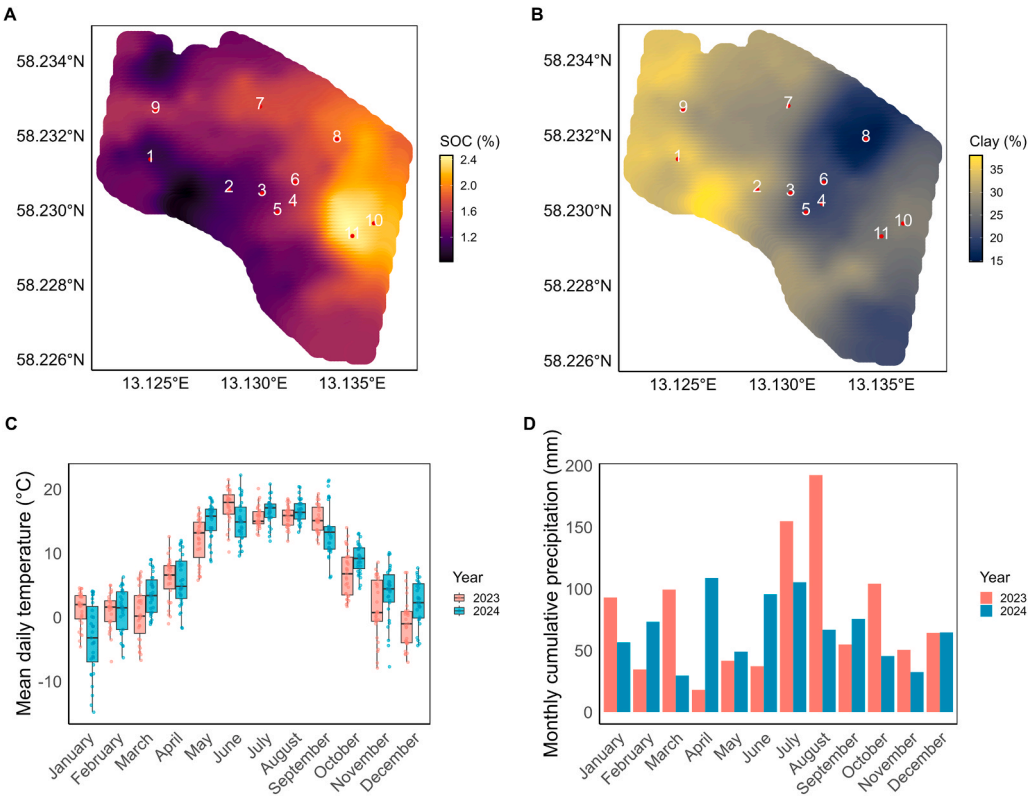

Fig. 1. Maps of the field in Bjertorp, Sweden, showing the sampled locations in 2023 and 2024 and the spatial variation in topsoil properties: (A) soil organic carbon content and (B) clay content at 3–13 cm depth. Box plots illustrate (C) mean daily temperature (each box shows the distribution of mean day temperatures for that month) and (D) monthly cumulative precipitation, based on interpolated gridded data from Swedish Meteorological and Hydrological Institute (SMHI).

Table 1
Descriptive statistics for the variables used for the 11 sampling locations used in the current study. Data was derived from Fukumasu et al. (2021) taken at 3 – 13 cm depth. SD is the standard deviation, and CV is the coefficient of variation.

Variable	Units	Means	SD	Minimum	Maximum	Median	CV
Soil organic carbon content	mg g^{-1}	16.9	4.3	11.8	24.3	15.1	25.2
Elevation	m (above sea level)	92.9	2.7	87.7	95.4	94.5	2.9
Clay content	%	28.1	7.6	16.5	38.8	30.3	26.9

2.4. Shoot and root sampling

Shoot samples were collected in one 50 cm × 50 cm area at each location using an electric clipper. The shoot samples were cut approximately 1 cm above the soil surface. The shoot samples were oven-dried at 60°C for 48 h within one day of collection. Root samples were taken at the depths 0–20 and 20–40 cm in the same grid as the shoot samples. Four sampling points were randomly chosen per sampling location: two samples between and two within the rows (Schuurman and Goedewaagen, 1971). Samples were taken using a metal auger with an inner diameter of 7 cm. Samples were stored in sealed polyethene bags at −20°C until further processing.

2.5. Separation of roots and root biomass determination

Root biomass was determined using an adapted version of the method described in Mattila and Häkkinen (2025). Roots were first soaked overnight in a mixture of water and 100–200 mL of perfume-free liquid soap (Mölndal, Sweden) in closed buckets at 4°C. Following soaking, the soil was removed using a power hose, and remaining organic matter residues and any residual soil particles were repeatedly rinsed and sifted through a 1 mm sieve until all soil aggregates had disintegrated to minimize any losses (Böhm, 1979). Once all visible aggregates had been broken down, organic matter was separated from sand and gravel by density and transferred to a colorless container to which water was added. The mixture was continuously stirred, and floating organic matter was extracted using a 50 μm sieve. This process was repeated 5–10 times, depending on the volume of organic matter. The material collected on the 50 μm sieve was transferred to 70 % ethanol for storage until further analysis. Roots were then visually identified using a 127 mm glass lens magnifying lamp with a 570-lumen LED light by color and root architectural properties, and separated using tweezers (Böhm, 1979). Roots were stored in 70 % ethanol at 4°C until further analysis. All root fragments smaller than about 5 mm were excluded for practical reasons before scanning or removed from the images during post-processing. Finally, the roots were dried at 60°C for 48 h and weighed.

2.6. Root imaging and image processing

Roots were scanned in a flatbed scanner (Epson Perfection V850, Tokyo, Japan) at a resolution of 600 dpi. The roots were physically separated using plastic tweezers so that they did not exceed 1 cm of root length per cm^2 of tray area to minimize overlap (Delory et al., 2017). The final images were saved in tif-format and analyzed with RhizoVision Explorer Version 2.03 (Seethepalli et al., 2021) using the settings given

in Supplemental Table S4. Root length and volume measurements acquired with RhizoVision were used to calculate root length density (cm root cm^{-3} soil) and root tissue density (g root cm^{-3} dry root biomass). In addition, the median root diameter was determined from RhizoVision, and roots were assigned to diameter classes (very fine: 0–0.2 mm, fine: 0.2–2 mm, and small to large: >2 mm).

2.7. Quantification of plant traits

We calculated the root biomass by summing root biomass within and between rows according to Frasier et al. (2016) and adapted by Hirte et al. (2021) as follows:

$$RB_{within} = \frac{M_{within}}{\pi * \left(\frac{d}{2}\right)^2} * \frac{d}{s} \quad \text{(i)}$$

$$RB_{between} = \frac{M_{between}}{\pi * \left(\frac{d}{2}\right)^2} * \frac{s-d}{s} \quad \text{(ii)}$$

where RB_{within} (g m^{-2}) and $RB_{between}$ (g m^{-2}) denote root biomass within and between rows respectively, M_{within} (g) and $M_{between}$ (g) denote the dry weight of roots extracted from the soil cores taken within and between rows respectively, d (m) is the inner diameter of the auger, and s (m) is the distance between rows. The shoot biomass per area, SB (g m^{-2}), was determined by:

$$SB = \frac{M}{A_Q} \quad \text{(iii)}$$

where M (g) is the dry weight of the shoots, and A_Q (m^2) is the sampled area. Measured shoot and root biomass (0–40 cm) data were then used to calculate root-to-shoot ratios.

2.8. Statistics and data visualization

We used non-parametric rank tests to analyse the data since the variables were generally not normally distributed, and the sample size was relatively small (n = 11) (Table S2). Spearman's rank correlation coefficients (ρ) were used to assess all correlations. Field variation was characterized with median values and the quartile coefficient of variation (QCV). The QCV was calculated as the ratio of the difference between the third and first quartiles to their sum, expressed as a percentage (Bonett, 2006). Comparisons between years were conducted using the Wilcoxon signed-rank test. To explore temporal trends, scatter plots were used for measurements taken at the same locations in both years, with a 1:1 reference line included to facilitate visual comparison. Additionally, the geostatistical interpolation in Fig. 1A-B was performed applying ordinary kriging at a spatial resolution of 10 m with SOC and clay content data from Lindahl et al. (2008) for the field.

All data processing and statistical analyses were conducted using R version 4.3.1 (R Core Team, 2023). Root image data extracted from RhizoVision were aggregated using weighted means using the "combinefeature" function (Seethepalli et al., 2024). Data processing and structuring were performed using "tidyverse" (Wickham et al., 2019) and "dplyr" (Wickham, Bryan., 2023). Data visualization was carried out using "ggplot2" (Wickham, 2016), with additional enhancements for statistical plots provided by "ggpubr" (Kassambara, 2023). Correlation matrices were visualized using custom functions built with the "corrplot" package (Wei and Simko, 2021). For geospatial analyses, vector data were managed using the "sf" package (Pebesma, 2018), and raster outputs were generated and masked to field boundaries using "terra" (Hijmans, 2023). Geostatistical interpolation was performed with "gstat" (Gräler et al., 2016). Field boundaries and the slope were digitized using Google Maps and Earth, respectively.

3. Results

3.1. Root and shoot biomass and the corresponding root-to-shoot ratio

Shoot biomass differed significantly between 2023 and 2024 ($p < 0.05$; QCV = 10 %; Fig. 2 A). Root biomass showed a similar pattern, with larger values in 2024 than in 2023 over the entire sampling depth (0–40 cm; Fig. 2B). Specifically, root biomass was 127 ± 24 g m^{-2} (median) in 2023 (QCV = 9 %; 0–40 cm; Fig. 2B) and 150 ± 40 g m^{-2} (median) in 2024 (QCV = 19 %; 0–40 cm; Fig. 2B). No significant differences in root biomass were found between years in the 20–40 cm layer or for the total 0–40 cm profile ($p > 0.05$; Fig. 2B). In contrast, root biomass in the top 20 cm was significantly larger in 2024 than in 2023 ($p < 0.05$; 0–20 cm; Fig. 2B). Across both years, 70–92 % of total root biomass was in the upper 20 cm, increasing from 2023 to 2024 (Fig. S1A). There was no significant overall effect of year on the root-to-shoot ratio ($p > 0.05$), with median values of 0.16 ± 0.04 in both years (Fig. 2 C). However, variation in root-to-shoot ratio was greater in 2023 (QCV = 18 %; Fig. 2 C) than in 2024 (QCV = 7 %; Fig. 2 C).

The shoot biomass, root biomass over the entire sampling depth, and root-to-shoot ratios in 2023 and 2024 were not correlated (Fig. 2D-F). Although there was a general tendency for both shoot and total root biomass to increase from 2023 to 2024, some locations showed notable decreases (Fig. 2 A, B). Relative increases were up to 70 and 200 % for shoots and total roots, respectively (Fig. S1A, B). Additionally, no consistent pattern was observed in the root-to-shoot ratio, with decreases up to 54 % and increases of more than 120 % (Fig. 2 F; Fig. S1C).

3.2. Root diameter, root tissue density and root length density

Root traits showed both notable within-field (QCVs up to 20 %; Table S2, S3) and temporal variation (Fig. 3A-C). Roots consistently had a higher median diameter in 2023 (QVC=4 %) than in 2024 (QVC=4 %) ($p < 0.05$; 0–40 cm; Fig. 3A). At 0–20 cm depth, the median root diameter was 0.29 ± 0.02 mm (QCV = 3 %; Fig. 3A) in 2023 and 0.27 ± 0.02 mm in 2024 (QCV = 4 %; Fig. 3A). A similar pattern was evident at 20–40 cm, where median root diameter decreased ($p < 0.05$) from 0.34 ± 0.02 mm in 2023 (QCV = 4 %) to 0.29 ± 0.04 mm in 2024 (QCV = 10 %). Across all depths and years, the majority (up to 98 %) of roots had diameters smaller than 2 mm, while roots thicker than 2 mm contributed less than 1 % to the total length (Fig. S3).

Root length density (RLD) exhibited notable variation within the field (QCV up to 24 %; Tables S2, S3) and differed significantly between years ($p < 0.05$; Fig. 3B). At 0–20 cm depth, median RLD was 13.0 ± 3.38 cm cm^{-3} in 2023 (QCV = 15 %) and was significantly smaller ($p < 0.05$) than in 2024, where values were 17.4 ± 5.33 cm cm^{-3} (QCV = 15 %). The same trend was observed at 20–40 cm depth as at 0–20 cm depth, with a wider variation in 2023 (QCV = 24 %) and 2024 (QCV = 16 %).

Root tissue density (RTD) also displayed considerable within-field variation (QCV up to 20 %; Tables S2, S3), with values ranging from 0.05 to 0.09 g cm^{-3} . However, no significant differences in RTD were observed between years ($p > 0.05$; Fig. 3C). At 0–20 cm depth, median RTD ranged from 0.07 ± 0.01 g cm^{-3} in 2023 (QCV = 7 %) and 0.07 ± 0.01 g cm^{-3} in 2024 (QCV = 9 %). Median RTD values were similar at the 20–40 cm depth.

Root diameter, root length density (RLD), and root tissue density (RTD) in 2023 and 2024 were not correlated to each other (Fig. 3D-F). Relative decreases in root diameter from 2023 to 2024 were up to 20 % (Fig. S2A), while RLD and RTD increased up to 200 and 30 %, respectively (Fig. S2B, C).

3.3. Correlations between soil properties and root traits across years in the top 20 cm

There were generally more significant correlations between soil

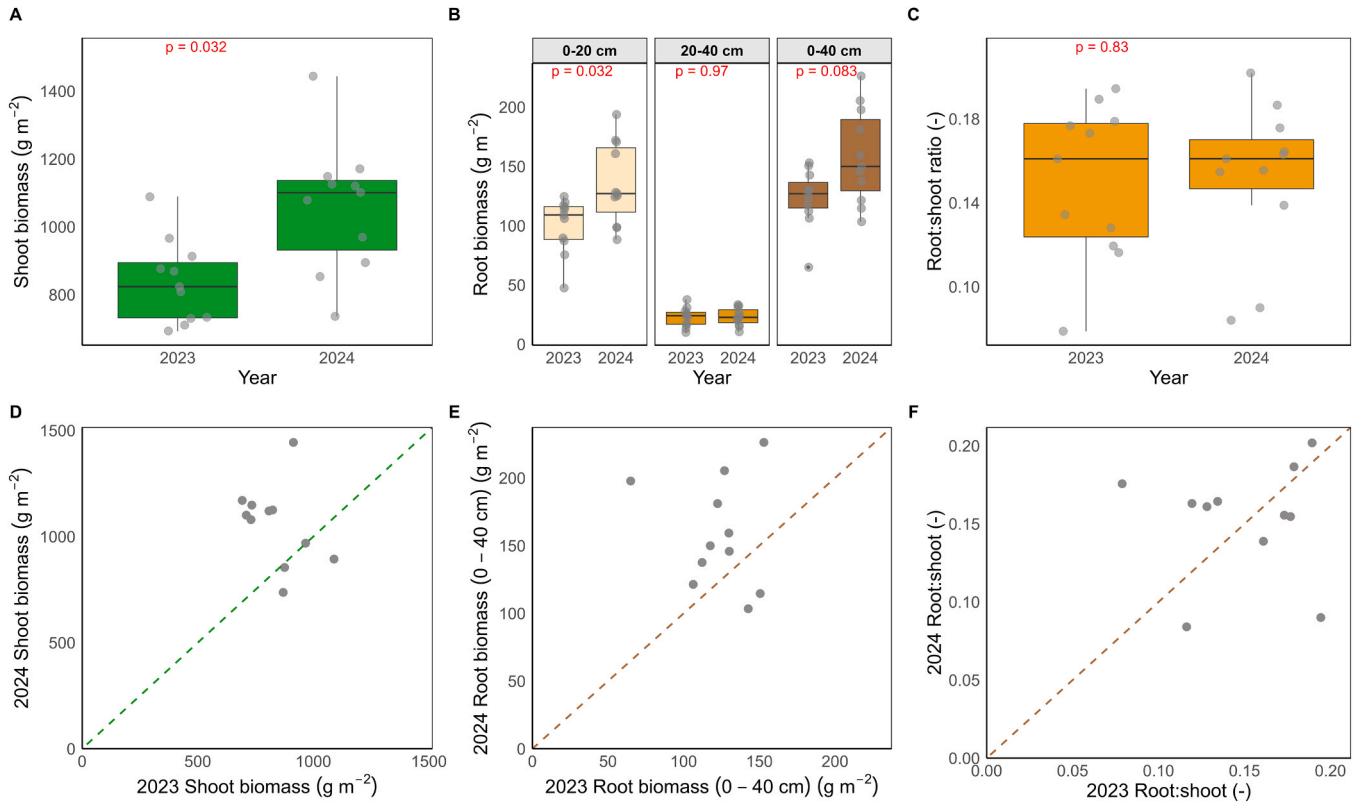

Fig. 2. (A) Total shoot biomass (g m^{-2}), (B) root biomass by depth (g m^{-2}), and (C) root-to-shoot ratio in study years 2023 and 2024. P-values indicate significance levels from the Wilcoxon signed-rank test. Between-year comparison of the (D) shoot biomass, (E) total root biomass and (F) root-to-shoot ratio, where the 1:1 line denotes equal values between years and deviations from this line illustrate the absence of a consistent relationship between 2023 and 2024 sampled at early to mid-reproductive stage, i.e. milking/early dough development stage (BBCH 71–83).

properties and plant traits in the wetter year 2024 compared to 2023 in the top 20 cm (Fig. 4A-B). In 2023, RLD was negatively correlated with SOC content, while in 2024, shoot biomass was negatively correlated with clay content and root diameter and RTD were positively correlated with clay content (Fig. 4A-B). The mean root biomass in the top 20 cm for the two years was also uncorrelated with SOC content (Fig. 4A-B).

4. Discussion

Observed median root-to-shoot ratios in our study (0.16) align with values reported for spring barley in southern Finland (0.14; Pietola and Alakukku 2005), values for small-grain cereals in Central European (0.07–0.18; Hirte et al. (2021)) and North American agro-ecosystems (~0.13; Bolinder et al. (2007)), indicating broad consistency in magnitude across regions and methods. Across both years, 70–92 % of root biomass was contained in the upper 20 cm of the soil profile (Fig. 2B). This depth distribution is broadly consistent with prior reports for small-grain cereals: spring barley allocated approximately 59 % of total (0–60 cm) root biomass to the 0–20 cm layer under Finnish conditions (Pietola and Alakukku, 2005), 70–75 % of spring barley roots were found within 0–20 cm of the 0–100 cm profile in experiments sensitive to nitrogen fertilization (Hansson and Andrén, 1987), and spring annual crops, on average, had allocated about 13–92 % of the root biomass to the 0–20 cm portion of the 0–40 cm profile across Finnish systems (Mattila and Häkkinen, 2025).

4.1. Root-to-shoot ratios show large within-field variation

Here, we found substantial within-field variation in root-to-shoot ratios across both sampling years. The quartile coefficient of variation (QCV) was 18 % in 2023 and 7 % in 2024, with no consistent spatial pattern emerging between years (Fig. 2 F). This indicates that above-ground biomass was a poor predictor of SOC input via roots, even under uniform management and climate. Previous studies have reported even larger variation in root-to-shoot ratios across sites and broader spatial scales, where differences have been attributed to tillage practices, soil texture, nutrient availability, crop genotype, and climate conditions. These findings highlight the multifactorial nature of belowground carbon allocation in annual cereals (Bolinder et al., 2007, Heinemann et al., 2023, Hirte et al., 2021, Hu et al., 2018, Mattila and Häkkinen, 2025, Xu and Juma, 1992).

For instance, the range of root-to-shoot ratios, including only roots in the 0–20 cm depth observed in our study (0.06–0.16 in 2023; 0.07–0.17 in 2024) was much narrower than the values reported for annual grain crops in a regional study from Finland (0.01–2.27; Mattila and Häkkinen, 2025). Similarly, when considering roots down to 40 cm, QCVs of 40 % in 2021 and 54 % in 2023 were found across multiple farms and spring crops in Mattila and Häkkinen (2025), again exceeding the variation observed within our field.

In the study of Mattila and Häkkinen (2025), the strongest predictors of root-to-shoot ratios were depth to a compacted layer and clay content. However, within our field, root-to-shoot ratios were not correlated with SOC content, clay content, or elevation (Fig. 4), suggesting that other unmeasured variables governed the observed within-field variation. Moreover, the lack of correlation between years (Fig. 2 F) indicates that different factors may have been important in the drier year 2023 compared with 2024. Alternatively, the same variables may have interacted differently with climatic conditions, so that their relative influence shifted between the years.

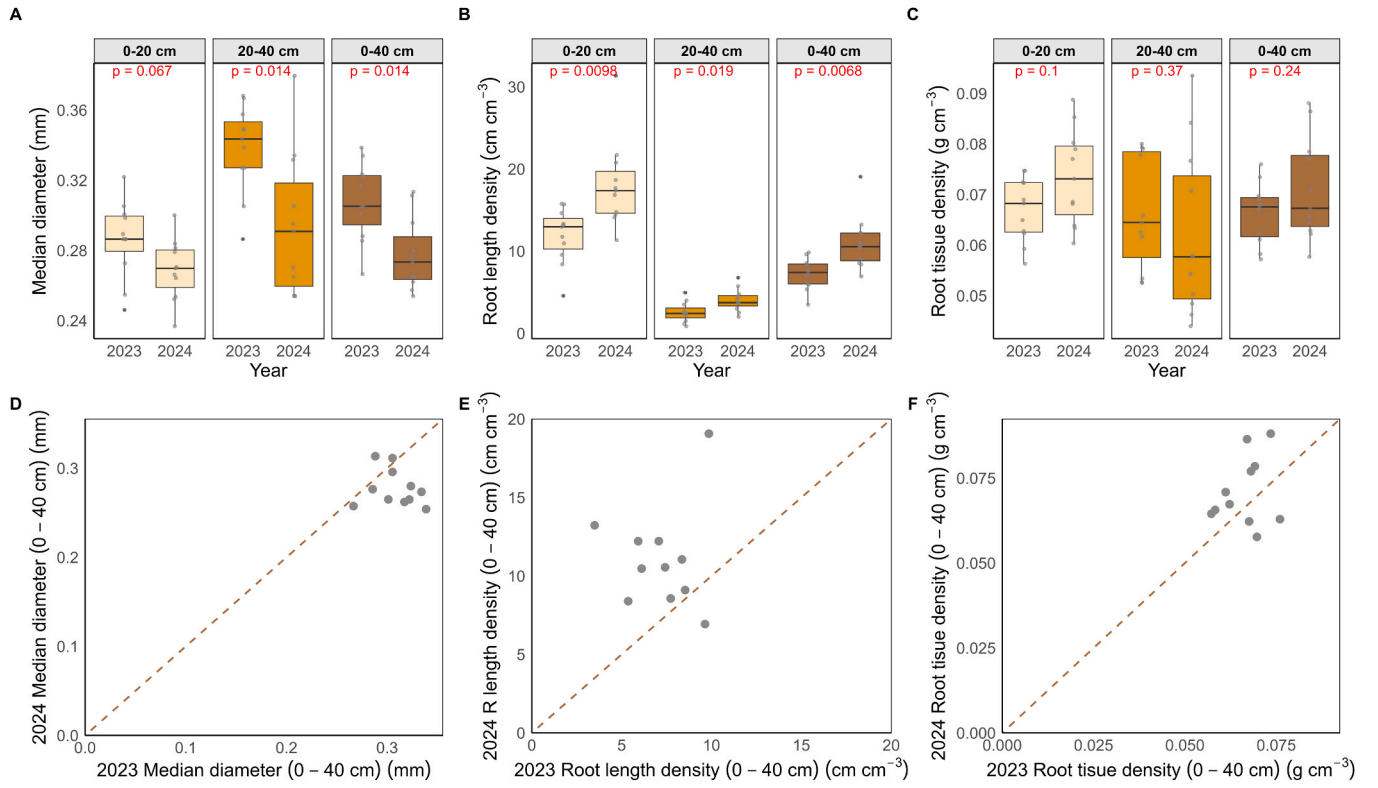

Fig. 3. A) Median root diameter, B) root length density, and C) root tissue density. P-values indicate significance levels from the Wilcoxon signed-rank test. Between-year comparison of the (D) shoot biomass, (E) root biomass and (F) root-to-shoot ratio, where the 1:1 line denotes equal values between years and deviations from this line illustrate the absence of a consistent relationship between 2023 and 2024 sampled at early to mid-reproductive stage, i.e. milking/early dough development stage (BBCH 71–83).

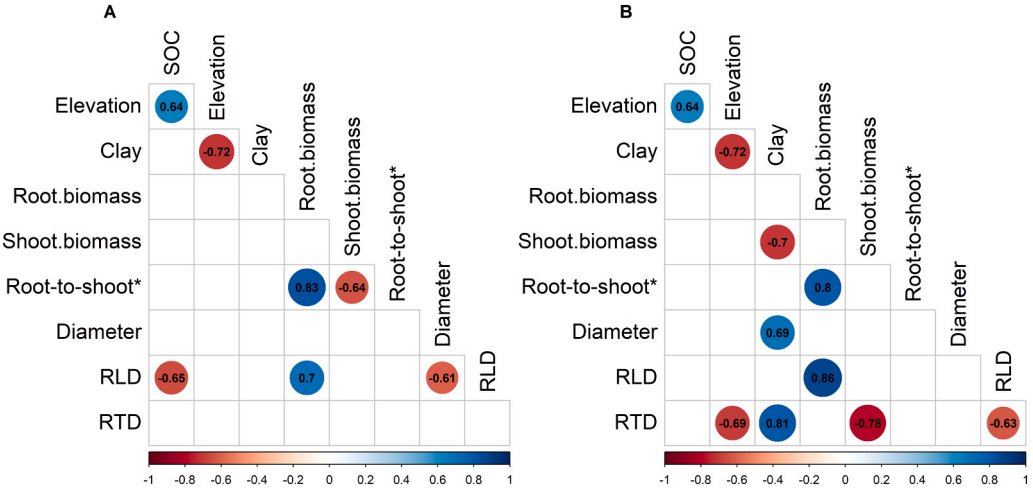

Fig. 4. Spearman rank correlation coefficients (ρ) between selected soil and site parameters measured in 2017 at 3–10 cm depth (Fukumasu et al., 2021) and root parameters at 3–10 cm for (A) 2023 and (B) 2024. Only statistically significant correlations ($p < 0.05$) are shown. SOC, soil organic carbon content; RLD, root length density; RTD, root tissue density. Root-to-Shoot* denotes the root-to-shoot ratio calculated using root biomass across the full measured depth (0–40 cm).

4.2. Shoot and root biomass differed between years

Inter-annual differences were evident in both shoot biomass and root biomass in the top 20 cm (Fig. 2 A, B), with topsoil biomass increasing from 2023 to 2024. These differences coincided with lower cumulative precipitation between April and June in 2023 (97.1 mm) compared with 2024 (254 mm), while mean temperatures were similar (~12 °C; Fig. 1C, D). The drier conditions in 2023 likely contributed to the reduced shoot and root biomass in the topsoil. In April 2023, the sowing month, had the lowest precipitation during the growing season (18.1 mm; Fig. 1D), which may have impaired crop productivity (Kaushal and Wani, 2016).

Although there was no significant overall effect of year on the root-to-shoot ratio, patterns varied considerably among sampling points (Fig. 2 F). This suggests that root-to-shoot ratio responses depended on field location, indicating interactive effects between site-specific soil properties and year-to-year weather conditions. Similar inter-annual effects have been reported elsewhere: in a four-year Danish study,

variation in root-to-shoot ratios of cereals was strongly linked to weather conditions, with dry springs associated with reduced topsoil root biomass and deeper root distribution (Hu et al., 2018). Likewise, Mattila and Häkkinen (2025) found that the proportion of roots in subsoil layers was partly determined by the number of early-season moisture stress days, with more subsoil allocation occurring in the year with higher moisture stress.

It remains uncertain whether differences in barley cultivars between the two years (Laureate in 2023 and Lexy in 2024) and the differences in the growth stage at the time of sampling (i.e. early to mid-reproductive stage at milking/early dough development stage) contributed to the observed inter-annual variation in shoot and root biomass and, thus, the root-to-shoot ratio. For instance, the effect of timing on root-to-shoot ratios has been documented in western Canada, producing a wide range of root-to-shoot ratios with time (Xu and Juma, 1992). However, this is unlikely to explain the differences observed here, as both cultivars (Lexy and Laureate) were sampled at similar growth stages. Additionally, cultivar-dependent variation at ripening ranged from 0.08 to 0.11 among four barley cultivars (Abee, Harrington, Bonanza and, Samson) (Xu and Juma, 1992), which may have contributed to the variation observed between Lexy and Laureate in this study. However, other studies have found root-to-shoot ratios to be broadly consistent among barley cultivars (Leger, Chapais and Codac) (Bolinder et al., 1997). In wheat, by contrast, considerable genotypic variation expressed in different cultivars and varieties has been reported, with coefficients of variation up to 45 % in spring wheat and 25 % in winter wheat (Heinemann et al., 2023).

4.3. Implications of the observed within-field variation in root and shoot data on SOC content

Although the majority of root biomass was concentrated in the upper 20 cm of the soil profile, we found no correlation between soil organic carbon (SOC) content and root biomass in either study year (Fig. 4) or when data from both years were averaged (Fig. S4). Previous research has established that root-derived inputs are among the most important factors in building up SOC (e.g., (Bolinder et al., 2007, Ogle et al., 2012, Börjesson et al., 2018). However, in our study, root inputs measured at the 0–20 cm depth did not explain SOC content in the topsoil. Three main factors likely contributed to this result:

First, there was substantial year-to-year variation in root biomass at most field locations, and two years of sampling were insufficient to generate representative mean values of root inputs. For comparison, a previous long-term study at this site found a correlation (ρ=0.49) between SOC and mean relative yield (the ratio of site-specific grain yield to the field's average yield, used as a proxy for total plant carbon inputs from both roots and above-ground residues) for 14 years in the period 1997–2016 (Fukumasu et al., 2021). Notably, mean relative yield correlated negatively with both elevation and clay content, suggesting reduced carbon inputs in lower-lying, clay-rich areas due to sub-optimal crop growth. In contrast, our measurements of root and shoot biomass did not reveal similar patterns. Second, we did not account for carbon inputs from rhizodeposition, such as sloughed-off root cells and exudates, which can amount to roughly 65 % of below-ground carbon (Bolinder et al., 2007). Third, SOC contents are not only determined by carbon inputs but on the long-term balance between input and losses, primarily through microbial decomposition.

Despite pronounced variation in clay content, SOC, and elevation across the field (Fig. 1A–B), the sources of variation in root-to-shoot ratios remain unresolved. These ratios were uncorrelated between years (Fig. 2 F), suggesting that unmeasured local properties played an important role and that their effects on root-to-shoot ratios varied between the two seasons, which experienced contrasting early-season precipitation.

4.4. Root diameter, root tissue density and root length density varied between years and soil depth

Root tissue density (RTD) showed within-field variation (QCV 6–20 %) across years. Although no significant interannual differences were detected, differences in changes per sampling location were observed (Fig. 3F). Notably, in the wetter year of 2024, but not in 2023, RTD in the top 20 cm was positively associated with clay content and negatively correlated with elevation (Fig. 4A-B). This suggests that RTD was affected by interactive effects between the weather and localized soil conditions. Median root diameters showed limited within-field variation (QCV = 4 %) and were larger during the drier year of 2023, ranging from 0.27 to 0.34 mm, compared to 2024 (0.25–0.31 mm) and tended to become larger with depth (Fig. 3B and E). These results suggest that the increase in diameter was a response to increased soil mechanical resistance, which typically increases in drier soil and in lower soil layers with greater bulk density (Vanhees et al., 2022, Potocka and Szymanowska-Pułka, 2018).

Similarly, the larger mean root diameter in the topsoil at sites with higher clay content in 2024 (Fig. 4) likely reflects greater mechanical resistance in soils with higher clay content. Increased penetration resistance also decreases root branching (Potocka and Szymanowska--Pułka, 2018, Lynch, 2022). Both root thickening and reduced branching lead to increased mean root diameter. In our study, we cannot separate these two possible effects. Such variation and the plastic nature of root diameter, even at this scale, are critical for trait-to-trait conversions, such as RTD and specific root length, as well as for robust model parameterization (Pagès and Kervella, 2018, Rose, 2017, Freschet et al., 2020, Jarvis et al., 2024, Hansen et al., 2012).

Root length density ranged from 3.5 to 9.9 cm cm^{-3} in 2023 and increased twofold in 2024 (Fig. S1B) and showed considerable within-field variation with a QCV of 16–24 %. Our data from 2023 align with reported values for spring barley under medium and high sowing densities and other temperate cereals (Gregory, 2006). The range of RLD values in 2024 (6.9–19 cm cm^{-3}) was comparable to grasses that have an RLD of about 20 cm cm^{-3} or more (Stokes et al., 2009). Improved understanding of the source of this variation in the RLD, could improve the parametrization of SOC models. In these predictive models, such as the USSF model (Jarvis et al., 2024), RLD is modelled to dictate where organic matter is supplied within the soil profile, especially when it is combined with the root depth distribution (Freschet et al., 2020, Coucheney et al., 2024, Poirier et al., 2018).

5. Conclusions

The large within-field variability in shoot and root biomass, root-to-shoot ratios and root traits at early to mid-reproductive stage, together with differences in both mean values and spatial patterns between the two study years, indicate that the use of fixed root-to-shoot ratios for estimating root carbon inputs may introduce substantial uncertainty into SOC model predictions. The observed variability in root biomass and root traits highlights their plasticity in response to environmental conditions. Recognizing and accounting for spatial heterogeneity in root traits is crucial, as these dynamics should be reflected in SOC model parameterization, even at the scale of individual fields. The current scarcity of comprehensive root trait datasets that demonstrate plasticity in response to environmental conditions is a key limitation in SOC modelling, reinforcing the need for expanded empirical research.

CRediT authorship contribution statement

Tino Colombi: Writing – review & editing, Validation, Supervision, Methodology, Conceptualization. **Thomas Kätterer:** Writing – review & editing, Validation, Supervision. **Mats Larsbo:** Writing – review & editing, Writing – original draft, Validation, Supervision, Methodology, Funding acquisition, Conceptualization. **Miyanda Chilipamushi:**

Writing – review & editing, Writing – original draft, Visualization, Validation, Software, Methodology, Investigation, Formal analysis, Data curation. **Claudia von Brömssen:** Writing – review & editing, Validation, Supervision, Methodology.

Funding sources

This study was financed by the FORMAS (grant no. 01326, 2020). TC also acknowledges funding from the University of Nottingham (Nottingham Research Fellowship) and TK from FORMAS (grant no. 00214, 2022).

Declaration of Generative AI and AI-assisted technologies in the writing process

During the preparation of this work, the author(s) used Perplexity in order to edit the grammar. After using this tool/service, the author(s) reviewed and edited the content as needed and take(s) full responsibility for the content of the publication.

Declaration of Competing Interest

The authors declare that they have no known competing financial interests or personal relationships that could have influenced the work reported in this paper.

Acknowledgments

We would like to thank Kjell Carlsson at Lantmännen for support with sampling in Bjertorp. We would also thank Nick Jarvis for valuable comments on the first draft of this manuscript. We also extend our gratitude to Sajani Hansana and Keron Bwacha for their assistance with root selection and scanning. We would also like to thank Tuomas Mattila for generously making his data available for comparison with our study.

Appendix A. Supporting information

Supplementary data associated with this article can be found in the online version at doi:10.1016/j.still.2026.107103.

Data availability

Data will be made available on request.

References

Asefa, M., Worthy, S.J., Cao, M., Song, X., Lozano, Y.M., Yang, J., 2022. Above- and below-ground plant traits are not consistent in response to drought and competition treatments. Ann. Bot. 130, 939–950. https://doi.org/10.1093/aob/mcac108.

Bao, Y., Aggarwal, P., Robbins, N.E., Sturrock, C.J., Thompson, M.C., Tan, H.Q., Tham, C., Duan, L., Rodriguez, P.L., Vernoux, T., Mooney, S.J., Bennett, M.J., Dinneny, J.R., 2014. Plant roots use a patterning mechanism to position lateral root branches toward available water. Proc. Natl. Acad. Sci. U. S. A. 111, 9319–9324. https://doi.org/10.1073/pnas.1400966111.

Böhm, W., 1979. Methods of studying root systems. Ecol. Stud. https://doi.org/10.1007/978-3-642-67282-8.

Bolinder, M., Angers, D., Dubuc, J., 1997. Estimating shoot to root ratios and annual carbon inputs in soils for cereal crops. Agric. Ecosyst. Environ. 63, 61–66. https://doi.org/10.1016/S0167-8809(96)01121-8.

Bolinder, M., Menichetti, L., Lundblad, M., Kätterer, T., 2019. Implementing a new version of ICBM in NIR. ⟨https://urn.kb.se/resolve?urn=urn:nbn:se:naturvardsverket:diva-8932⟩.

Bolinder, M., Janzen, H., Gregorich, E., Angers, D., VandenBygaart, A., 2007. An approach for estimating net primary productivity and annual carbon inputs to soil for common agricultural crops in Canada. Agric. Ecosyst. Environ. 118, 29–42. https://doi.org/10.1016/j.agee.2006.05.013.

Bonett, D.G., 2006. Confidence interval for a coefficient of quartile variation. Comput. Stat. Data Anal. 50, 2953–2957. https://doi.org/10.1016/j.csda.2005.05.007.

Börjesson, G., Bolinder, M.A., Kirchmann, H., Kätterer, T., 2018. Organic carbon stocks in topsoil and subsoil in long-term ley and cereal monoculture rotations. Biol. Fertil. Soils 54, 549–558. https://doi.org/10.1007/s00374-018-1281-x.

Cabal, C., De Deurwaerder, H.P.T., Matesanz, S., 2021. Field methods to study the spatial root density distribution of individual plants. Plant Soil 462, 25–43. https://doi.org/10.1007/s11104-021-04841-z.

Coleman, K., Jenkinson, D., 2014. RothC – A model for the turnover of carbon in soil. Model description and users guide (Windows version, updated June 2014). ⟨https://repository.rothamsted.ac.uk/item/98xv8/rothc-a-model-for-the-turnover-of-carbon-in-soil-model-description-and-users-guide-windows-version-updated-june-2014⟩.

R. Core Team, 2023. R: A language and environment for statistical computing. R Foundation for Statistical Computing, Vienna, Austria. ⟨https://www.R-project.org⟩.

Coucheney, E., Herrmann, A.M., Jarvis, N., 2024. A simple model of the turnover of organic carbon in a soil profile: model test, parameter identification and sensitivity. EGUsphere 2024 1–22. https://doi.org/10.5194/egusphere-2024-3883.

Delory, B.M., Weidlich, E.W.A., Meder, L., Lütje, A., Van Duijnen, R., Weidlich, R., Temperton, V.M., 2017. Accuracy and bias of methods used for root length measurements in functional root research. Methods Ecol. Evol. 8, 1594–1606. https://doi.org/10.1111/2041-210X.12771.

Dupuy, L., Gregory, P.J., Bengough, A.G., 2010. Root growth models: towards a new generation of continuous approaches. J. Exp. Bot. 61, 2131–2143. https://doi.org/10.1093/jxb/erp389.

Durand-Maniclas, F., Heinemann, H., Seidel, F., Ciulla, F., Bárcena, T.G., Camenzind, M., Corrado, S., Csűrös, Z., Czakó, Z., Eylenbosch, D., Ficke, A., Flamm, C., Herrera, J.M., Horáková, V., Hund, A., Lüddeke, F., Platz, F., Poós, B., Rasse, D., Hirte, J., 2025. Linking root length and surface area to yield: variety-specific root plasticity in winter wheat across contrasting European environments. Ann. Bot. https://doi.org/10.1093/aob/mcaf155.

Frasier, I., Noellemeyer, E., Fernández, R., Quiroga, A., 2016. Direct field method for root biomass quantification in agroecosystems. MethodsX 3, 513–519. https://doi.org/10.1016/j.mex.2016.08.002.

Freschet, G.T., Roumet, C., Comas, L.H., Weemstra, M., Bengough, A.G., Rewald, B., Bardgett, R.D., De Deyn, G.B., Johnson, D., Klimešová, J., Lukac, M., McCormack, M. L., Meier, I.C., Pagès, L., Poorter, H., Prieto, I., Wurzburger, N., Zadworny, M., Bagniewska-Zadworna, A., Stokes, A., 2020. Root traits as drivers of plant and ecosystem functioning: current understanding, pitfalls and future research needs. N. Phytol. 232, 1123–1158. https://doi.org/10.1111/nph.17072.

Fukumasu, J., Poeplau, C., Coucheney, E., Jarvis, N., Klöffel, T., Koestel, J., Kätterer, T., Svensson, D.N., Wetterlind, J., Larsbo, M., 2021. Oxalate-extractable aluminum alongside carbon inputs may be a major determinant for organic carbon content in agricultural topsoils in humid continental climate. Geoderma 402, 115345. https://doi.org/10.1016/j.geoderma.2021.115345.

Gasser, A.A., Diel, J., Nielsen, K., Mewes, P., Engels, C., Franko, U., 2022. A model ensemble approach to determine the humus building efficiency of organic amendments in incubation experiments. Soil Use Manag 38, 179–190. https://doi.org/10.1111/sum.12699.

Gräler, B., Pebesma, E., Heuvelink, G., 2016. Spatio-temporal interpolation using gstat. R. J. 8, 204–218. https://doi.org/10.32614/RJ-2016-014.

Gregory, P., 2006. Roots, rhizosphere and soil: the route to a better understanding of soil science? Eur. J. Soil Sci. 57, 2–12. https://doi.org/10.1111/j.1365-2389.2005.00778.x.

Gregory, P.J., Palta, J.A., Batts, G.R., 1996. Root systems and root:mass ratio – carbon allocation under current and projected atmospheric conditions in arable crops. Plant Soil 187, 221–228. ⟨http://www.jstor.org/stable/42947907⟩.

Hansen, S., Abrahamsen, P., Petersen, C.T., Styczen, M.E., 2012. Daisy: model use, calibration, and validation. Trans. ASABE 55, 1317–1335. https://doi.org/10.13031/2013.42244.

Hansson, A.C., Andrén, O., 1987. Root dynamics in barley, lucerne and meadow fescue investigated with a mini-rhizotron technique. Plant Soil 103, 33–38. https://doi.org/10.1007/BF02370664.

Heinemann, H., Hirte, J., Seidel, F., Don, A., 2023. Increasing root biomass derived carbon input to agricultural soils by genotype selection – a review. Plant Soil 490, 19–30. https://doi.org/10.1007/s11104-023-06068-6.

Heinemann, H., Durand-Maniclas, F., Seidel, F., Ciulla, F., Bárcena, T.G., Camenzind, M., Corrado, S., Csűrös, Z., Czakó, Z., Eylenbosch, D., Ficke, A., Flamm, C., Herrera, J.M., Horáková, V., Hund, A., Lüddeke, F., Platz, F., Poós, B., Rasse, D., Don, A., 2025. Optimising root and grain yield through variety selection in winter wheat across a European climate gradient. Eur. J. Soil Sci. 76. https://doi.org/10.1111/ejss.70077.

Hijmans, R.J., 2023. terra: Spatial data analysis. ⟨https://rspatial.org⟩.

Hirte, J., Leifeld, J., Abiven, S., Oberholzer, H.R., Hammelehle, A., Mayer, J., 2017. Overestimation of Crop Root Biomass in Field Experiments Due to Extraneous Organic Matter. Mar 1 Front Plant Sci. 8, 284. https://doi.org/10.3389/fpls.2017.00284.

Hirte, J., Leifeld, J., Abiven, S., Oberholzer, H., Mayer, J., 2018. Below ground carbon inputs to soil via root biomass and rhizodeposition of field-grown maize and wheat at harvest are independent of net primary productivity. Agric. Ecosyst. Environ. 265, 556–566. https://doi.org/10.1016/j.agee.2018.07.010.

Hirte, J., Walder, F., Hess, J., Büchi, L., Colombi, T., van der Heijden, Mayer, J., 2021. Enhanced root carbon allocation through organic farming is restricted to topsoils. Sci. Total Environ. 755, 143551. https://doi.org/10.1016/j.scitotenv.2020.143551.

Hoad, S.P., Russell, G., Lucas, M.E., Bingham, I.J., 2001. The management of wheat, barley, and oat root systems. Adv. Agron. 74, 193–246. https://doi.org/10.1016/S0065-2113(01)74034-5.

Hu, T., Sørensen, P., Wahlström, E.M., Chirinda, N., Sharif, B., Li, X., Olesen, J.E., 2018. Root biomass in cereals, catch crops and weeds can be reliably estimated without considering aboveground biomass. Agric. Ecosyst. Environ. 251, 141–148. https://doi.org/10.1016/j.agee.2017.09.024.

IUSS Working Group, W.R.B., 2015. World Reference Base for Soil Resources 2014, update 2015. In: International soil classification system for naming soils and creating legends for soil maps. World Soil Resources Reports, 106. FAO, Rome.
Jacobs, A., Poeplau, C., Weiser, C., Fahrion-Nitschke, A., Don, A., 2020. Exports and inputs of organic carbon on agricultural soils in Germany. Nutr. Cycl. Agroecosyst 118, 249–271. https://doi.org/10.1007/s10705-020-10087-5.
Jarvis, N., Coucheney, E., Lewan, E., Klöffel, T., Meurer, K.H.E., Keller, T., Larsbo, M., 2024. Interactions between soil structure dynamics, hydrological processes, and organic matter cycling: a new soil–crop model. Eur. J. Soil Sci. 75. https://doi.org/10.1111/ejss.13455.
Kassambara, A., 2023. ggpubr: 'ggplot2' based publication ready plots. R package version 0.6.0. ⟨https://CRAN.R-project.org/package=ggpubr⟩.
Kätterer, T., Bolinder, M.A., Andrén, O., Kirchmann, H., Menichetti, L., 2011. Roots contribute more to refractory soil organic matter than above-ground crop residues, as revealed by a long-term field experiment. Agric. Ecosyst. Environ. 141, 184–192. https://doi.org/10.1016/j.agee.2011.02.029.
Kaushal, M., Wani, S.P., 2016. Rhizobacterial–plant interactions: strategies ensuring plant growth promotion under drought and salinity stress. Agric. Ecosyst. Environ. 231, 68–78. https://doi.org/10.1016/j.agee.2016.06.031.
Khan, M., Gemenet, D.C., Villordon, A., 2016. Root system architecture and abiotic stress tolerance: current knowledge in root and tuber crops. Front. Plant Sci. 7, 1584. https://doi.org/10.3389/fpls.2016.01584.
Lantmännen, 2025. Inför vårsådd 2025: Vårutsäde, vallfrö, majs, mellan- och fånggrödor för svenska odlingsförhållanden. ⟨https://www.lantmannenlantbrukmaskin.se/siteassets/om-oss/vara-tjanster/broschyrtorg/spannmal-och-vaxtodling/infor-varsadd-2025_.pdf⟩ (accessed 28 January 2026).
Lindahl, A.M., Söderström, M., Jarvis, N., 2008. Influence of input uncertainty on prediction of within-field pesticide leaching risks. J. Contam. Hydrol. 98, 106–114. https://doi.org/10.1016/j.jconhyd.2008.03.006.
Liski, J., Palosuo, T., Peltoniemi, M., Sievänen, R., 2005. Carbon and decomposition model Yasso for forest soils. Ecol. Model 189, 168–182. https://doi.org/10.1016/j.ecolmodel.2005.03.005.
Lux, A., Rost, T.L., 2012. Plant root research: the past, the present and the future. Ann. Bot. 110, 201–204. https://doi.org/10.1093/aob/mcs156.
Lynch, J.P., 2022. Harnessing root architecture to address global challenges. Plant J. 109, 415–431. https://doi.org/10.1111/tpj.15560.
Mattila, T.J., Häkkinen, L., 2025. Exploring the effects of soil structure, nutrients, and farm management on crop root biomass and depth distribution. Field Crops Res 327, 109909. https://doi.org/10.1016/j.fcr.2025.109909.
O'Leary, G., Liu, D., Ma, Y., Li, F., McCaskill, M., Conyers, M., Dalal, R., Reeves, S., Page, K., Dang, Y., 2015. Modelling soil organic carbon. 1. The value of long term agronomic experimental data. ⟨https://www.cabidigitallibrary.org/doi/10.5555/20183347100⟩.
Messing, I., Soriano, A.M.M., Svensson, D.N., Barron, J., 2024. Variability and compatibility in determining soil particle size distribution by sieving, sedimentation and laser diffraction methods. Soil Tillage Res 238, 105987. https://doi.org/10.1016/j.still.2023.105987.
Ogle, S.M., Swan, A., Paustian, K., 2012. No-till management impacts on crop productivity, carbon input and soil carbon sequestration. Agric. Ecosyst. Environ. 149, 37–49. https://doi.org/10.1016/j.agee.2011.12.010.
Pagès, L., Kervella, J., 2018. Seeking stable traits to characterize the root system architecture. Study on 60 species located at two sites in natura. Ann. Bot. 122, 107–115. https://doi.org/10.1093/aob/mcy061.
Pebesma, E., 2018. Simple features for R: standardized support for spatial vector data. R. J. 10, 439–446. ⟨https://journal.r-project.org/archive/2018/RJ-2018-009⟩.
Pietola, L., Alakukku, L., 2005. Root growth dynamics and biomass input by Nordic annual field crops. Agric. Ecosyst. Environ. 108, 135–144. https://doi.org/10.1016/j.agee.2005.01.009.
Plaza-Bonilla, D., Álvaro-Fuentes, J., Hansen, N.C., Lampurlanés, J., Cantero-Martínez, C., 2013. Winter cereal root growth and aboveground–belowground biomass ratios as affected by site and tillage system in dryland Mediterranean conditions. Plant Soil 374, 925–939. https://doi.org/10.1007/s11104-013-1926-3.
Poirier, V., Roumet, C., Munson, A.D., 2018. The root of the matter: linking root traits and soil organic matter stabilization processes. Soil Biol. Biochem 120, 246–259. https://doi.org/10.1016/j.soilbio.2018.02.016.
Potocka, I., Szymanowska-Pułka, J., 2018. Morphological responses of plant roots to mechanical stress. Ann. Bot. 122, 711–723. https://doi.org/10.1093/aob/mcy010.
Rasse, D.P., Rumpel, C., Dignac, M., 2005. Is soil carbon mostly root carbon? Mechanisms for a specific stabilisation. Plant Soil 269, 341–356. https://doi.org/10.1007/s11104-004-0907-y.
Raza, S., Cooper, H.V., Girkin, N.T., Kent, M.S., Bennett, M.J., Mooney, S.J., Colombi, T., 2025. Missing the input: the underrepresentation of plant physiology in global soil carbon research. SOIL 11, 363–369. https://doi.org/10.5194/soil-11-363-2025.
Rose, L., 2017. Pitfalls in root trait calculations: how ignoring diameter heterogeneity can lead to overestimation of functional traits. Front. Plant Sci. 8, 898. https://doi.org/10.3389/fpls.2017.00898.
Schuurman, J.J., Goedewaagen, M.A.J., 1971. Methods for the examination of root systems and roots. Pudoc, Wageningen.
Seethepalli, A., Dhakal, K., Griffiths, M., Guo, H., Freschet, G.T., York, L.M., 2021. RhizoVision Explorer: open-source software for root image analysis and measurement standardization. AoB Plants 13, plab056. https://doi.org/10.1093/aobpla/plab056.
Seethepalli, A., Ottley, C., Childs, J., Cope, K.R., Fine, A.K., Lagergren, J.H., Kalluri, U., Iversen, C.M., York, L.M., 2024. Divide and conquer: using RhizoVision Explorer to aggregate data from multiple root scans using image concatenation and statistical methods. N. Phytol. 244, 2101–2108. https://doi.org/10.1111/nph.20151.
Seidel, S.J., Ahmadi, S., Weihermüller, L., Couedel, A., Lopez, G., Behrend, D., Kamali, B., Gaiser, T., Hernández-Ochoa, I., 2024. The overlooked effects of environmental impacts on root:shoot ratio in experiments and soil-crop models. Sci. Total Environ. 955, 176738. https://doi.org/10.1016/j.scitotenv.2024.176738.
Stokes, A., Atger, C., Bengough, A.G., Fourcaud, T., Sidle, R.C., 2009. Desirable plant root traits for protecting natural and engineered slopes against landslides. Plant Soil 324, 1–30. https://doi.org/10.1007/s11104-009-0159-y.
Taghizadeh-Toosi, A., Christensen, B.T., Hutchings, N.J., Vejlin, J., Kätterer, T., Glendining, M., Olesen, J.E., 2014. C-TOOL: a simple model for simulating whole-profile carbon storage in temperate agricultural soils. Ecol. Model 292, 11–25. https://doi.org/10.1016/j.ecolmodel.2014.08.016.
Vanhees, D.J., Schneider, H.M., Sidhu, J.S., Loades, K.W., Bengough, A.G., Bennett, M.J., Pandey, B.K., Brown, K.M., Mooney, S.J., Lynch, J.P., 2022. Soil penetration by maize roots is negatively related to ethylene-induced thickening. Plant Cell Environ. 45, 789–804. https://doi.org/10.1111/pce.14175.
Watt, M., Magee, L.J., McCully, M.E., 2008. Types, structure and potential for axial water flow in the deepest roots of field-grown cereals. N. Phytol. 178, 135–146. https://doi.org/10.1111/j.1469-8137.2007.02358.x.
Weemstra, M., Freschet, G.T., Stokes, A., Roumet, C., 2021. Patterns in intraspecific variation in root traits are species-specific along an elevation gradient. Funct. Ecol. 35, 342–356. https://doi.org/10.1111/1365-2435.13723.
Weemstra, M., Valverde-Barrantes, O.J., McCormack, M.L., Kong, D., 2022. Root traits and functioning: from individual plants to ecosystems. Oikos 2023, e09924. https://doi.org/10.1111/oik.09924.
Wei, T., Simko, V., 2021. corrplot: visualization of a correlation matrix. R. Package Version 0. 92. ⟨https://github.com/taiyun/corrplot⟩.
Wickham, H., 2016. Programming with ggplot2. ggplot2: Elegant graphics for data analysis. Springer, Cham, pp. 241–253. https://doi.org/10.1007/978-3-319-24277-4_12.
Swedish Meteorological and Hydrological Institute (SMHI). Gridded Precipitation and Temperature Data (PTHBV). ⟨https://www.smhi.se/data/ladda-ner-data/griddade-nederbord-och-temperaturdata-pthbv⟩ (accessed 25 August 2025).
Wickham, H., Bryan, J., 2023. R packages. O'Reilly Media, Sebastopol, CA.
Wickham, H., Averick, M., Bryan, J., Chang, W., McGowan, L.D.A., François, R., Grolemund, G., Hayes, A., Henry, L., Hester, J., Kuhn, M., Pedersen, T.L., Miller, E., Bache, S.M., Müller, K., Ooms, J., Robinson, D., Seidel, D.P., Spinu, V., Yutani, H., 2019. Welcome to the tidyverse. J. Open Source Softw. 4, 1686. https://doi.org/10.21105/joss.01686.
Xu, J.G., Juma, N.G., 1992. Above- and below-ground net primary production of four barley (Hordeum vulgare L.) cultivars in western Canada. Can. J. Plant Sci. 72, 1131–1140. https://doi.org/10.4141/cjps92-138.